Reproductive Sciences (2020) 27:940–953
https://doi.org/10.1007/s43032-019-00098-1

ORIGINAL ARTICLE

Declining BRCA-Mediated DNA Repair in Sperm Aging and its Prevention by Sphingosine-1-Phosphate

Robert Stobezki[1] · Shiny Titus[1] · Dorota Halicka[2] · Zbigniew Darzynkiewicz[2] · Kutluk Oktay[1]

Received: 14 May 2019 / Accepted: 17 July 2019 / Published online: 8 January 2020

Abstract

Recent data suggest that paternal age can have major impact on reproductive outcomes, and with increased age, there is increased likelihood of chromosomal abnormalities in the sperm. Here, we studied DNA damage and repair as a function of male aging and assessed whether sphingosine-1-phosphate (S1P), a ceramide-induced death inhibitor, can prevent sperm aging by enhancing DNA double-strand breaks (DSB) repair. We observed a significant increase in DNA damage with age and this increase was associated with a decline in the expression of key DNA DSB repair genes in mouse sperm. The haploinsufficiency of BRCA1 male mice sperm showed significantly increased DNA damage and apoptosis, along with decreased chromatin integrity when compared to similar age wild type (WT) mice. Furthermore, haploinsufficiency of BRCA1 male mice had lower sperm count and smaller litter size when crossed with WT females. The resulting embryos had a higher probability of growth arrest and reduced implantation. S1P treatment decreased genotoxic-stress-induced DNA damage in sperm and enhanced the expressions of key DNA repair genes such as BRCA1. Co-treatment with an ATM inhibitor reversed the effects of S1P, implying that the impact of S1P on DNA repair is via the ATM-mediated pathway. Our findings indicate a key role for DNA damage repair mechanism in the maintenance of sperm integrity and suggest that S1P can improve DNA repair in sperm. Further translational studies are warranted to determine the clinical significance of these findings and whether S1P can delay male reproductive aging.

Summary

There is mounting evidence that sperm quality declines with age, similar to that of the oocyte. However, the reasons behind this decline are poorly understood and there is no medical intervention to improve sperm quality. Our study suggests a strong role for DNA damage repair in maintenance of sperm quality, and for the first time, a potential pharmaceutical approach to prevent sperm aging

Keywords Aging · Gene expression · Sperm · DNA fragmentation

Introduction

Age plays a key role in the reproductive potential of both sexes. It has been well established in females that fertility and oocyte quality decline with age, essentially precluding live births after ages 45–46 and resulting in significant increase in chromosomal abnormalities in the preceding decade [1]. We have recently shown that BRCA-related DNA repair pathways may play a key role in oocyte aging [2]. We found that ATM-mediated DNA repair function declines with age in human oocytes, which renders them more susceptible to genotoxic stress and results in the increasing accumulation of DNA damage [2].

Although less apparent than in females, recent research indicates that men also show significant signs of reproductive aging. Sperm counts display age-related decline [3],

Electronic supplementary material The online version of this article (https://doi.org/10.1007/s43032-019-00098-1) contains supplementary material, which is available to authorized users.

✉ Kutluk Oktay
info@fertilitypreservation.org

[1] Department of Obstetrics and Gynecology, Laboratory of Molecular Reproduction and Fertility Preservation, Yale University School of Medicine, 310 Cedar Street, FMB Room # 224, New Haven, CT 06510, USA

[2] Department of Pathology and Brander Cancer Research Institute, New York Medical College, Valhalla, NY 10595, USA

chromosomal abnormalities and DNA fragmentation increase in sperm with age [4–6]. Sperm from older men, especially when female partner is also older than 40 years of age, contribute to infertility [7, 8]. Moreover, the incidence of schizophrenia, autism, and autosomal dominant diseases are increased among children born from older men [9]. It is unclear if this chromosomal damage is initiated in spermatogonial stem cells or it accumulates in germ cells during spermatogenesis; however, aging seems to coincide with the number of DSBs in human sperm [10, 11].

With a significant trend in delaying childbearing both in men [12, 13] and women [14], male reproductive aging could adversely affect an increasing proportion of children being born. Despite this prominent public health impact, little is known on the mechanism of male reproductive aging and methods to slow down this process.

In this study, we hypothesized that declining DNA repair may have a significant role in sperm aging akin to its role in oocytes. Furthermore, we sought to reverse this process with a ceramide-induced cell death suppressor sphingosine-1-phosphate (S1P).

S1P has been shown to prevent radiotherapy- and chemotherapy-induced oocyte death but the mechanism of its action is not fully understood [15, 16]. Because we have previously shown a common mechanism between chemotherapy- and age-induced oocyte death via the induction of DNA damage, we hypothesized that S1P may reduce gamete aging by contributing to more effective DNA repair. To study our hypothesis, we utilized aging male mice as well as those haploinsufficient for BRCA1.

Materials and Methods

The animal studies were carried out in strict accordance with the recommendations in the Guide for the Care and Use of Laboratory Animals of the U.S. National Institutes of Health (NIH) and the Institutional Animal Care and Use Committee at New York Medical College. All Friend's leukemia virus B (FVB) mice were purchased from Taconic. BRCA1 and mice were obtained from NCI Fredrick Mouse Repository. BRCA1 breeding colony was maintained and their offspring were genotyped.

Mating and Genotyping

In the BRCA1 breeding colony, wild type (WT) female mice were co-housed with heterozygous male mice. The litter sizes produced by the mating setup were recorded. BRCA1 transgenic mice were selected on the basis of their sensitivity to genotoxic stress [17] and obtained from the NIH Fredrick Mouse Repository. The mice were kept in a temperature- and light-regulated room environment; 12-h light/12-h dark cycle and bred in-house. BRCA1-mutant mice carried a deletion of 330 base pairs (bp) in intron 10 plus 407 bp in exon 11 of the BRCA1 gene ($BRCA1^{+/\Delta 11}$). Owing to the deletion, the $BRCA1^{\Delta 11}$ gene product is retained in the cytoplasm, which severely compromises its nuclear functions. $BRCA1^{\Delta 11/\Delta 11}$ mice were not viable and died at embryonic days 7 to 8; $BRCA1^{\Delta 11/\Delta 11}$ embryos exhibited both early post-implantation growth retardation and chromosomal abnormalities [17]. γ-Irradiation-induced Rad51 focus formation is impaired in cells in which only $BRCA1^{\Delta 11}$ was expressed [18].

After weaning, tail and ear biopsies were obtained and DNA was isolated for genotyping using the manufacturer's protocol. DNA was extracted by treating the biopsies with lysis buffer (Teknova) supplemented with proteinase K (Invitrogen) at 55 °C overnight. The following day, the DNA was precipitated with equal volumes of isopropanol. The pellet was washed in 70% ethanol and air-dried. After reconstitution with adequate amount of nuclease-free water, PCR was performed with gene-specific primers to identify the genotype (Table S1).

The primers used for identifying BRCA1 wild type were B004/B005, which amplifies a 450-bp fragment, and for BRCA1 heterozygous were B004/B007, which amplifies a 550-bp fragment [17]. The PCR reaction mixture consisted of a 10 μl total volume of 10 μl, containing 5 μl ImmoMix (Bioline), 1 μl of primer (Integrated DNA Technologies), 3 μl of nuclease free water, and 1 μl of DNA. Cycling conditions were 94 °C for 5 min, 35 cycles of 94 °C for 0.5 min, 58 °C for 1 min, and 72 °C for 45 s, followed by 72 °C for 10 min. Amplified products were run on 2% agarose gel electrophoresis, with ethidium bromide staining, and visualization with AlphaImager 2200 (Alpha Innotech) to determine the genotype.

Collection and Processing of Mouse Spermatozoa and Testis

Young (2–3-month-old) and reproductively senescing old (10–14-month-old) WT male mice and young (2–3-month-old) haploinsufficient BRCA1 mice were studied. Mice were euthanized via anesthesia and cervical dislocation. Testes were removed, fixed in 10% formaldehyde, embedded in paraffin, and serially sectioned for expression of γH2AX assessment by immunohistochemistry analysis. The cauda epididymis and vas deferens were excised surgically and placed into a 35-mm dish (Becton Dickinson) with M199 media (Corning). Mature spermatozoa were collected by parallel action of applying gentle pressure with forceps at one end of the vas deferens, and flushing with M199 media (Corning) with a 30-gauge needle. The needle was also used lengthwise along the epididymis to expel the sperm. Sperm were washed and manipulated using Multipurpose Handling Medium (Irvine Scientific). Sperm counts were calculated for each sample

collected using a hemocytometer. Sperm were either studied live or fixed for immunocytochemistry and immunofluorescence studies.

S1P, H_2O_2, and ATM Inhibitor Treatments

Male germ cells were exposed to 200 μM S1P with and without H_2O_2 (1 mM) in culture for 1 h [19]. In addition, an ATM inhibitor was utilized (10 μM) (KU-55593, Abcam) [16] in some experiments. We subsequently assessed DNA damage, apoptosis, and chromatin integrity and studied the DNA DSB repair gene expression by qRT-PCR in sperm lysates.

Immunohistochemistry and Immunofluorescence for DNA Damage Assessment

We utilized a Ser139 phosphorylation–specific γH2AX antibody (IHC-00059; Bethyl Laboratories) with enzymatic diaminobenzidine staining (Vector) to assess DNA damage in mouse testicular tissue (Fig. 1a). Histone H2AX, one of the several variants of the nucleosome core histone H2A, becomes phosphorylated on Ser139 in response to DSBs (γH2AX). Within seconds of DSB formation, γH2AX foci are formed at the site of DNA damage, which can be detected by confocal microscopy or immunohistochemistry to quantify DNA damage. Foci of γH2AX represent DDR in a 1:1 manner, enabling sensitive quantification of potential DSBs [20].

Sperm were assessed for DNA damage with antibody to γH2AX (613402; BioLegend) and secondary antibody Alexa Fluor 488 (A-11029; Invitrogen), followed by nuclear counterstaining with diamidino-2-phenylindole (DAPI; Fisher Scientific) (Fig. 1b). Green immunofluorescence for sperm samples was measured by FACScan flow cytometer (Becton-Dickinson) or by laser scanning cytometry, using 488 excitation laser [21].

DNA integrity of mouse sperm was assessed via flow cytometry using acridine orange (AO) staining [22]. AO fluoresces green when attached to native DNA, and fluoresces red when attached to fragmented DNA. Basically, after induction of denaturation by heat or acid, the denatured DNA (ssDNA) stains metachromatically red with AO while dsDNA stains green**.** When the sample has ≥ 50% green fluorescence, the sample is of good quality. Similarly, AO was used to assess sperm chromatin structure by measuring its intensity of fluorescence, which is the ratio of red/(red+green) yields the percentage of DNA fragmentation (also known as DNA fragmentation index, or DFI%). Semen samples with sperm chromatin structure assay (SCSA) value of less than or equal to 15% DFI were regarded to have low-level DNA fragmentation, samples having between 15% and less than or equal to 30% DFI value were regarded to have moderate DNA fragmentation, and samples having above 30% DFI were regarded as exhibiting high levels of DNA fragmentation [23].

Levels of activated caspases were detected in mouse sperm samples using fluorescein-labeled inhibitors of caspases (FLICA). FLICA passes through an intact plasma membrane and covalently binds to the active caspase; any unbound FLICA diffuses out of the cell and is washed away. As FLICA only binds to the active caspase, there is no interference from pro-caspases or inactive forms of the enzyme. The inhibitors were used with the appropriate controls according to the kit instructions provided by the manufacturer (ImmunoChemistry Technologies). A 150-fold stock solution of the poly-caspase FAM-FLICA was prepared in dimethylsulfoxide (DMSO). It was further diluted in phosphate-buffered saline (PBS) to yield a 30-fold working solution. Sperm samples (300 μl) were incubated at 37 °C for 1 h with 10 μl of the working solution and subsequently washed twice with PBS. After labeling with FLICA, 1% propidium iodide (PI) in PBS was used to assess dead cells. All samples were analyzed directly by flow cytometry using the FLICA assay to detect caspase activity [24, 25].

qRT-PCR From Mouse Sperm Lysates

Sperm pellets previously snap-frozen in PBS were thawed. RNA was extracted using the trizol method [26]. The quality and quantity of the RNA were measured with NanoDrop 2000 from Thermo Scientific. RNA (2 μg) from each sample was taken for reverse transcription with dTVN and N9 primers and SuperScript III reverse transcriptase, all procured from Invitrogen. The resulting cDNA was used to perform real-time qPCR with SYBR Green on an Applied Biosystems 7900HT Real-Time PCR machine was used. To determine the relative expression of various DNA repair genes in mouse sperm, we used the ΔΔCt method, which makes use of the expression of housekeeping genes. GAPDH was used as housekeeping gene. Primers were procured from Integrated DNA technologies (IDT) (Table S2).

Embryo Collection and Quality Assessment

BRCA1 WT female mice (2–3 month-old, $n = 7$) were superovulated with intraperitoneal administration of 5 IU PMSG (pregnant mare's serum gonadotropin, Sigma-Aldrich) followed 72 h later with 5 IU human chorionic gonadotropin (Calbiochem, San Diego, CA). Mice were cohoused (2 female per male mouse) with either a haploinsufficient BRCA1 or WT male. The morning after mating, also known as embryonic day 0.5 (E0.5), female mice were checked for the presence of a vaginal plug as an indicator of mating. Those females with confirmed plugs were separated. On day 5, embryos were flushed from the uterus and

observed for morphology. Implantation rate was also assessed using 1% Evans blue dye.

Neutral Comet Assay

Slides were prepared 48 h prior to experimentation by coating normal glass microscope slides with 500 μl normal melting point agar (NMPA, 0.5% w/v in PBS) solution and left to dry at room temperature for no less than 48 h. Once samples were obtained, 10 μl of mouse sperm suspension was mixed with 90 μl of 0.5% low melting point agar (LMPA). Then this 100 μl solution was added to the NMPA-coated slides. Coverslips were added and slides were placed on a metallic tray on ice and in the dark for 5 min. The cover slips were then removed and another layer of LMPA was added. Cover slips were subsequently replaced before the LMPA hardened. Slides were then kept in the dark on ice again for another 5 min. After 10 min, the cover slips were removed and slides were placed in staining jars containing ice-cold lysing solution (2.5 M NaCl, 100 mM EDTA, sodium N-laurylsacrosinate [SLS], [1% w/v] and 10 mM Trizma base pH 10, and 1% Triton-X-100 and 10% DMSO (immediately adding before use)) for 1 h at 4 °C in a dark place.

After this lysis step, the slides were washed three times for 5 min with the cold electrophoresis buffer (0.089 M Tris base, 0.089 M boric acid, and 2 mM EDTA [pH 8.3]), and then placed flatly in the electrophoresis tank face up for 30 min. This incubation period was used to achieve the unwinding of the DNA. Electrophoresis was then performed at 18 V for 60 min. After this, slides were washed twice in PBS for 5 min each. Before analysis could occur, the sperm within the slides needed to be fixed by two 10-min washes in ethanol, and then air drying at room temperature. Ethidium bromide (50 μl at 10 μg/ml in water) was then added on the slide and sealed with a cover slip. Slides were kept moist, wrapped in aluminum foil to prevent light exposure, and stored at 4 °C until analysis [27].

Alkaline Comet Assay

Slides were prepared 48 h prior to experimentation by coating normal glass microscope slides with 500 μl normal melting point agar (0.5% w/v in PBS) solution and left to dry at room temperature for no less than 48 h. Then, 10 μl of mouse sperm suspension was mixed with 90 μl of 0.5% LMPA. Then this 100 μl solution was added to the NMPA-coated slides. Coverslips were added and slides were placed on a metallic tray on ice and in the dark for 5 min. The cover slips were removed and a 90-μl layer of LMPA was added. Cover slips were subsequently replaced before the LMPA hardened. Slides were then kept in the dark on ice again for another 5 min. After 10 min, the cover slips were removed and slides were placed in staining jars containing ice-cold lysing solution (2.5 M NaCl, 200 mM NaOH, 100 mM EDTA, 10 mM Trizma Base, 1% Triton X-100 and 10% DMSO [pH 10]) for 1.5 h at 4 °C in a dark place.

After this lysis step, the slides were washed three times for 5 min with TE buffer (pH 8.0), and then placed flatly in the electrophoresis tank face up for 30 min to achieve the unwinding of the DNA. The alkaline electrophoresis buffer in this tank included 300 mM NaOH and 1 mM EDTA [pH 13]. This incubation period was used to achieve the alkaline unwinding of the DNA. Electrophoresis was then performed at 25 V, 300 mA for 30 min. After this, slides were washed twice in neutralization buffer (0.4 M Tris, pH 7.5) for 5 min each. Before analysis could occur, the sperm within the slides needed to be fixed by draining the slides well on paper towels and then subjecting them to two 10-min washes in ethanol, and then air drying at room temperature for 5 min. Ethidium bromide (50 μl at 10 μg/ml in water) was then added on the slide, and sealed with a cover slip. Slides were kept moist, wrapped in aluminum foil to prevent light exposure, and stored at 4 °C until analysis [28].

Comet Assay Analysis

Slides from both alkaline and neutral comets were imaged by fluorescence microscopy using a Nikon OPTIPHOT microscope. ImageJ was used for comet assay analysis, which calculated tail length, tail moment, and % of DNA in the tail. Each image used had a dark background and light comets. The comets were "on scale" for the calculations to be correct (the brightest pixels of interest were below 255 on an 8-bit scale). Camera noise subtraction, flat field correction, and a background subtraction on the images were conducted before running the comet assay plugin for ImageJ. To analyze the slides, an oval around the sperm head was drawn and calculated and then an oval around the sperm tail was drawn and calculated. Each comet had two lines of results: the first line was the head values and the values were as follows: *X* and *Y* were coordinates of the Centroid, XM and YM were coordinates of the Center of Mass, IntDen and RawIntDen were the same and were the integrated density, TailLen was the tail length, TailMoment was the tail moment, and %TailDNA was percentage of total DNA that was in the tail. The "Center of Mass" is the brightness-weighted average of *XY* coordinates of a selection. Center of Mass of the tail and Centroid of the head were used in calculating the tail length. The tail length as used here was the distance from the Centroid of the head to the Center of Mass of the tail. It was calculated as the Pythagorean distance between two points. The tail length variable is called CometLen in the code. TailMoment was the length of the tail times the integrated density of the tail. Percentage of DNA in the tail was the integrated density of the tail divided by the

integrated density of the tail plus the integrated density of the head times 100. The %TailDNA was used to compare the samples of each group [29].

Statistical Analysis

All analyses were performed in a blinded fashion. Experiments were repeated at least three times. The results were reported as means with standard errors of the mean. SPSS 17 for Windows package (SPSS Inc.) and Microsoft Excel were used for statistical analysis. To choose the appropriate statistical test, we performed Levene's test of homogeneity of variances ($P < 0.01$) and Kolmogorov-Smirnov test of normality ($P < 0.01$). Continuous data (presented as means ± SEM) were analyzed by Student's t test. The difference was considered statistically significant if the P value was less than 0.05. A p value of < 0.1 was accepted as an indication for a trend towards significance. All analyses were two-tailed.

Results

Age-Related DNA Damage in Testis and Mature Sperm

First, we studied whether the extent of constitutive level of DNA damage as represented by the presence of γH2AX, increases with age in testes. The data showed that expression of γH2AX in spermatogonium and spermatocytes was significantly increased with age in the testis (Fig. 1a, c) (young vs. old: 134.6 ± 8.9 vs.169.2 ± 3.0; $P = 0.003$, Student's t test). Likewise, expression of γH2AX was also increased with age in in sperm of WT mice (young vs. old: 4.6 ± 0.6 vs. 15.4 ± 3.5, $n = 12$; $P = 0.006$, Student's t test) (Fig. 1b, Fig. 2a).

This increase in DNA damage with age was accompanied by increased percentage of sperm cells showing increased susceptibility of DNA to denaturation assessed by the acridine orange assay [23, 30] (17.4 ± 5.3 vs. 32.6 ± 3.6, $n = 10$; $P = 0.027$, Student's t test) (Fig. 2b) and increased frequency of apoptotic cells defined by FLICA

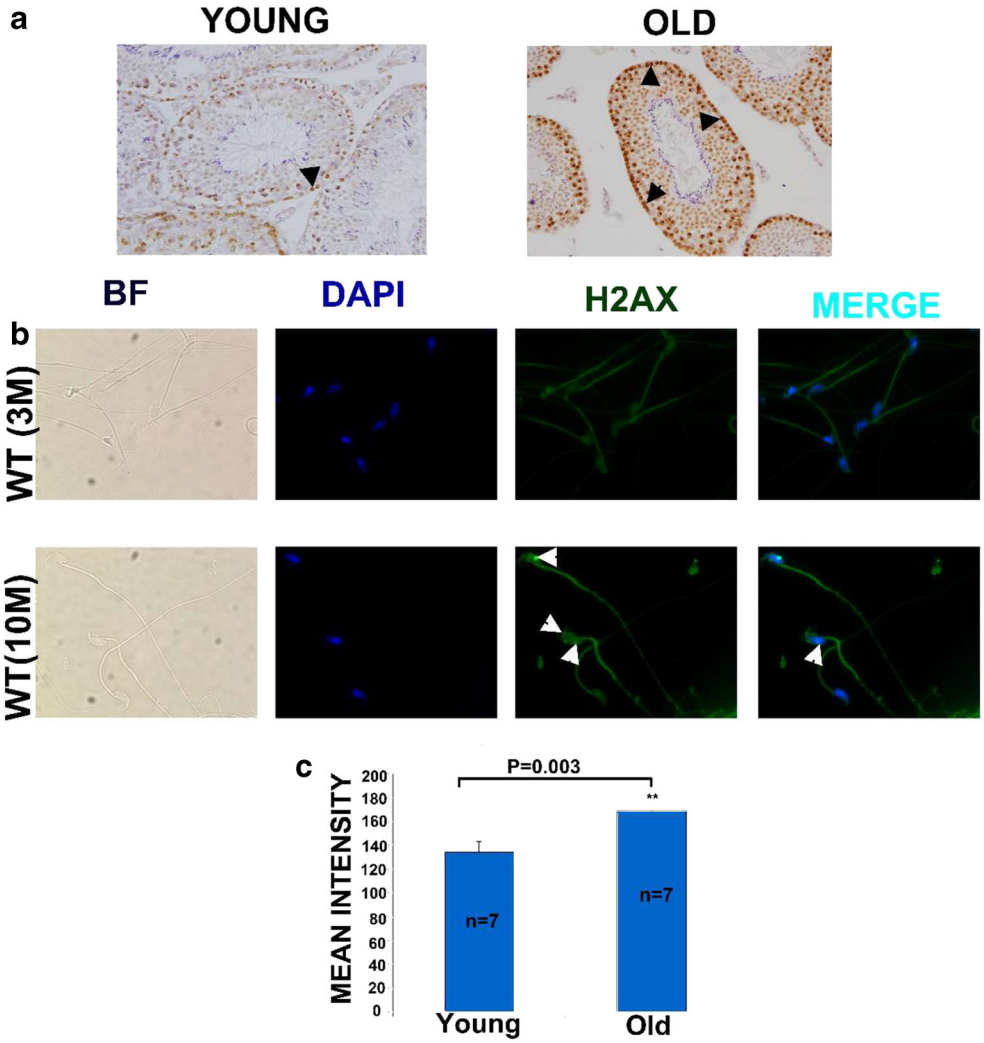

Fig. 1 Age-related DNA damage in testicular tissue and mature sperm cells. **a** Representative photomicrographs show γH2AX immunostaining of sperm cells of young and old mice at × 40 magnification. **b** Photomicrographs represent γH2AX foci (green) and counterstaining of DAPI (blue) of sperm cells from young and old WT mice at × 40 magnification. Arrowheads show increased numbers of γH2AX foci in old WT mice as compared to young WT mice. **c** Bar graph shows a higher expression of γH2AX as represented by the intensity of the γH2AX immunofluorescence in the spermatogonium and spermatocytes in testicular tissue of old (169.2 ± 3.0 vs. 134.6 ± 8.9, $n = 7$; $P = 0.003$; Student's t test) compared to young. All bar graphs show means ± SEM

analysis [24] (13.9 ± 1.5 vs. 35.5 ± 3.7, $n = 10$; $P = 7.9 \times 10^{-5}$, Student's t test) (Fig. 2c) as well as lower sperm cells count ($2.1 \times 10^6 \pm 0.07 \times 10^6$ vs. $1.7 \times 10^6 \pm 0.12 \times 10^6$, $n = 8$; $P = 0.05$, Student's t test) (Fig. 2d) as compared to the young. In addition, old male mice had smaller litter size when mated with young WT females compared to litter of young WT males mated with young WT females (young vs. old: 5.2 ± 0.72 vs. 6.9 ± 0.42, $n = 9$; $P = 0.05$, Student's t test) (Fig. 2e). These data established that aging may be associated with increased DNA damage and reduced fertility in male mice.

Haploinsufficiency of BRCA1

To probe the role of DNA damage repair efficiency in male reproductive aging, we studied young haploinsufficient BRCA1 mice [2]. We found that DNA DSBs were significantly increased compared to WT mice in spermatogonium and spermatocytes in the testis (155.2 ± 3.4 vs. 134.6 ± 8.9, $n = 7$; $P = 0.05$, Student's t test) (Fig. 3a) and in mature sperm from haploinsufficient BRCA1 mice by γH2AX expression (15.9 ± 4.3 vs. 4.6 ± 0.6, $n = 12$; $P = 0.03$, Student's t test) (Fig. 3b). This increase in DNA damage in the haploinsufficient BRCA1 mice was accompanied by increased percentage of DNA fragmentation (30.6 ± 3.4 vs. 17.4 ± 5.3, $n = 10$; $P = 0.05$, Student's t test) (Fig. 3c), apoptosis (30.7 ± 5.4 vs. 13.9 ± 1.5, $n = 10$; $P = 0.014$, Student's t test) (Fig. 3d), and lower sperm concentration compared to the WT ($1.8 \times 10^6 \pm 0.1 \times 10^6$ vs. $2.1 \times 10^6 \pm 0.07 \times 10^6$, $n = 8$; $P = 0.045$, Student's t test) (Fig. 3e). In addition, haploinsufficiency of BRCA1 male mice resulted in smaller litter size when mated with WT females compared to when WT males were mated with WT females (3.2 ± 0.77 vs. 6.9 ± 0.42, $n = 9$; $P = 0.0008$, Student's t test) (Fig. 3f).

Since we observed smaller litter sizes originating from haploinsufficient BRCA1 male mice, we explored the mechanism of this compromise. We evaluated embryogenesis by crossing BRCA1 WT mice with WT females and haploinsufficient BRCA1 male mice with WT females. We then counted the implantation sites as well as observing embryogenesis after in vivo fertilization. We found that implantation sites were significantly decreased in WT females crossed with B haploinsufficient BRCA1 male mice (0.43 ± 0.30 vs. 6.60 ± 2.34, $n = 7$; $P = 0.05$, Student's t test) when compared to crossing with WT males (Fig. 3g). We also observed a higher percentage of embryos arresting in blastocyst stage instead of hatching in WT females after mating with haploinsufficient BRCA1 male mice compared to mating with WT males (32.14% ± 0.13% vs. 8.33% ± 0.07%, $n = 7$; $P = 0.026$, Student's t test) (Fig. 3h). These data indicated that intact DNA DSB repair is important in maintaining sperm quality.

Decreased Expression of DSB Repair Genes in Aged and Haploinsufficient BRCA1 Mice

Because we found that the DNA damage was increased both with age and in haploinsufficient BRCA1 mice, we hypothesized that observed changes were due to age-related decline in efficiency of DSB repair in sperm. To study our hypothesis, we measured the expression of key ATM-mediated DSB repair genes by qRT-PCR in young and old mouse sperm. We found that the expression of BRCA1 (0.05 ± 0.01 vs. 0.04 ± 0.001, $P = 0.048$, Student's t test), ATM (0.011 ± 0.003 vs. 0.006 ± 0.002, $P = 0.014$, Student's t test), MRE11 (0.6 ± 0.3 vs. 0.1 ± 0.05, $P = 0.041$, Student's t test), DMC1 (0.008 ± 0.004 vs. 0.002 ± 0.004, $P = 0.036$, Student's t test), RAD50 ($2.2 \times 10^{-4} \pm 5 \times 10^{-5}$ vs. $9.2 \times 10^{-5} \pm 8 \times 10^{-5}$, $P = 0.028$, Student's t test), and RAD51 (0.3 ± 0.4 vs. 0.01 ± 0.4, $P = 0.0009$, Student's t test), declined significantly in old as compared to young WT mice (Fig. 4a–f).

Interestingly, in the haploinsufficient BRCA1 young mouse, the expressions of key DNA repair genes were similarly low as in old WT mice. These included BRCA1 (0.028 ± 0.012 vs. 0.05 ± 0.01, $P = 0.019$, Student's t test), ATM (0.002 ± 0.0005 vs. 0.011 ± 0.003, $P = 0.006$, Student's t test), MRE11 (0.045 ± 0.018 vs. 0.6 ± 0.3, $P = 0.02$, Student's t test), DMC1 ($0.002 \pm 9 \times 10^{-4}$ vs. 0.008 ± 0.004, $P = 0.02$, Student's t test), RAD50 ($9.7 \times 10^{-5} \pm 8.9 \times 10^{-6}$ vs. $2.2 \times 10^{-4} \pm 5 \times 10^{-5}$, $P = 0.044$, Student's t test), RAD51 ($0.002 \pm 8 \times 10^{-4}$ vs. 0.03 ± 0.4, $P = 0.015$, Student's t test) in haploinsufficient BRCA1 male mice when compared to similar age young WT mice (Fig. 5a–f). In fact, the expression levels of the DNA repair genes in the young haploinsufficient BRCA1 mice were similar to, and for some genes, even lower, than the expressions seen in the old WT mice. This data indicates that sperm aging may be accelerated in haploinsufficient BRCA1 mice.

Effect of S1P-Treatment on Mouse Sperm Chromosomal Integrity and Expression of DNA DSB Repair Genes

To determine if S1P can reduce DSBs by enhancing DNA repair and potentially reduce sperm aging, we subjected mouse sperm to H_2O_2 exposure in the presence or absence of S1P. We observed a significant decrease in expression of γH2AX with S1P and genotoxic stress as compared to H_2O_2 alone (8.29 ± 1.45 vs. 13.42 ± 1.51, $n = 9$; $P = 0.025$, Student's t test) (Fig. S1A). Treatment with S1P had no effect on the percentage of apoptosis, by FLICA (Fig. S1C), as well as susceptibility of DNA to denaturation by AO staining (Fig. S1E).

S1P treatment induced the expression of BRCA1 compared to baseline (0.471 ± 0.602 vs. 0.068 ± 0.031, $n = 9$; $P = 0.005$, Student's t test) and H_2O_2-treated sperm (0.755 ±

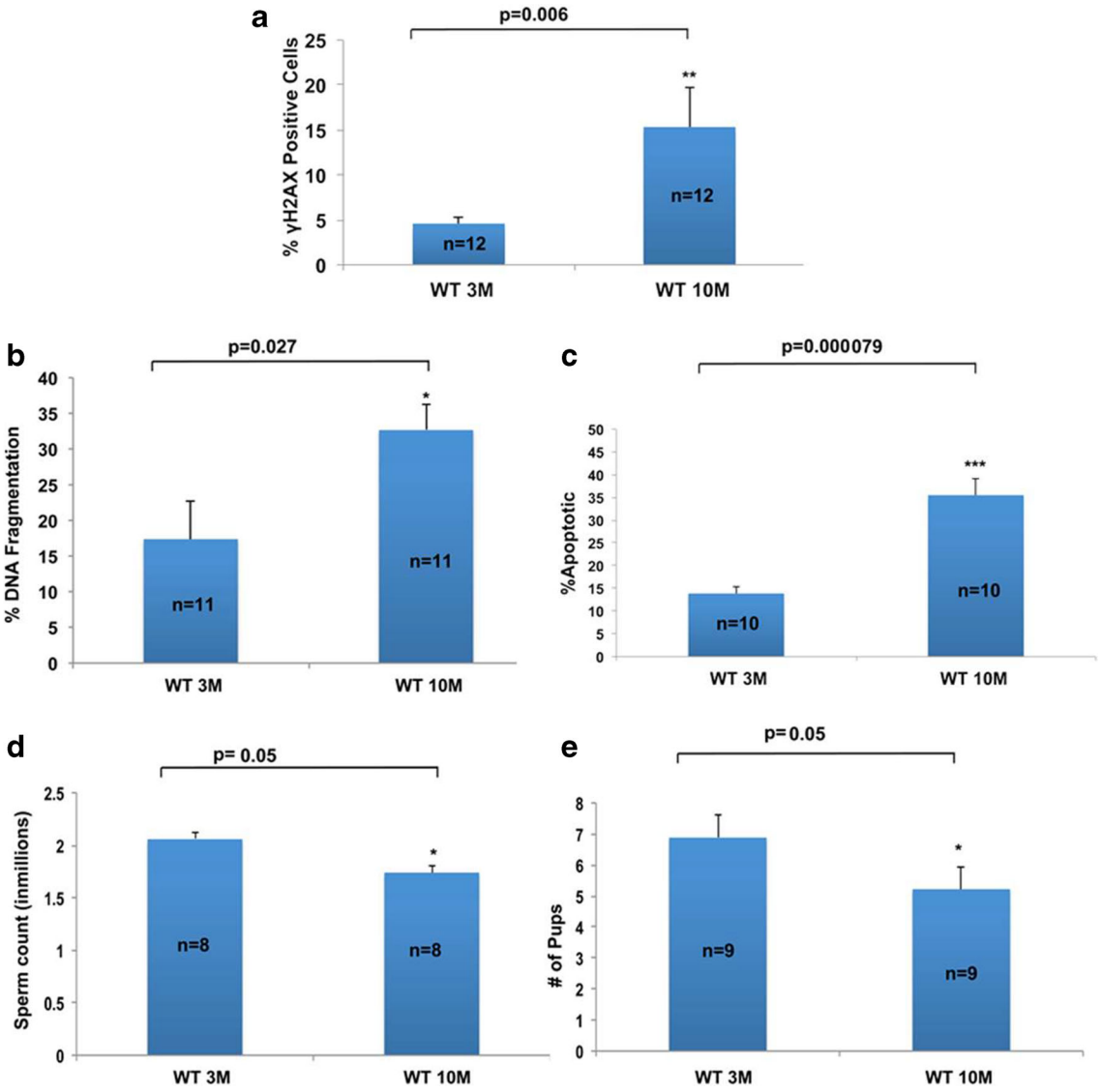

Fig. 2 Age-related decline in sperm quality. Aged mice showed an **a** increase in DNA damage as reported by γH2AX expression through utilizing laser scanning cytometry with at least 1000 cells counted per sample (4.6 ± 0.6 vs. 15.4 ± 3.5, $n = 12$; $P = 0.006$, Student's t test), **b** increased susceptibility of DNA of sperm cells to denaturation by the acridine orange assay (17.4 ± 5.3 vs. 32.6 ± 3.6, $n = 10$; $P = 0.027$, Student's t test), **c** increased percentage of apoptotic cells detected by the FLICA analysis (13.9 ± 1.5 vs. 35.5 ± 3.7, $n = 10$; $P = 7.9 \times 10^{-5}$, Student's t test), and **d** lower sperm concentration ($2.1 \times 10^6 \pm 0.07 \times 10^6$ vs. $1.7 \times 10^6 \pm 0.12 \times 10^6$, $n = 8$; $P = 0.05$, Student's t test) as compared to young. **e** Old male mice resulted in smaller litter size when mated with WT females compared to when WT males were mated with WT females (young vs. old: 5.2 ± 0.72 vs. 6.9 ± 0.42, $n = 9$; $P = 0.05$, Student's t test). All bar graphs show the means ± SEM

0.377 vs. 0.090 ± 0.053, $n = 9$; $P = 0.002$ Student's t test). Furthermore, there was a trend for increase in the expression of Rad51 (0.036 ± 0.015 vs. 0.012 ± 0.008, $n = 9$; $P = 0.07$, Student's t test) and DMC1 (0.016 ± 0.02 vs. 0.003 ± 0.002, $n = 9$; $P = 0.06$, Student's t test) in the S1P-treated samples when compared to the controls. S1P treatment did not have an effect on other tested genes when compared to the control (Fig. 6a–f).

To confirm that S1P reduces DNA damage in sperm via enhancing the actions of ATM-mediated DSB repair pathway, we replicated the above experiments with an ATM inhibitor co-treatment. The ATM inhibitor co-treatment reversed the benefits of S1P on DNA repair as shown by no change in DSBs via γH2AX expression (Fig. S1B) and percentage of apoptosis by FLICA (Fig. S1D), as well as susceptibility of DNA to denaturation by AO staining (Fig. S1F).

ATM inhibition also blocked or reversed the S1P-induced increase in the expression of DSB repair genes in the face of genotoxic stress. While the expressions of BRCA1, ATM, RAD50, and MRE11 did not increase with S1P treatment when an ATM inhibitor was used, interestingly, S1P suppressed the expressions of RAD51 (0.015 ± 0.056 vs. 0.052 ± 0.012, $n = 8$; $P = 0.05$, Student's t test) and DMC1 (0.0035

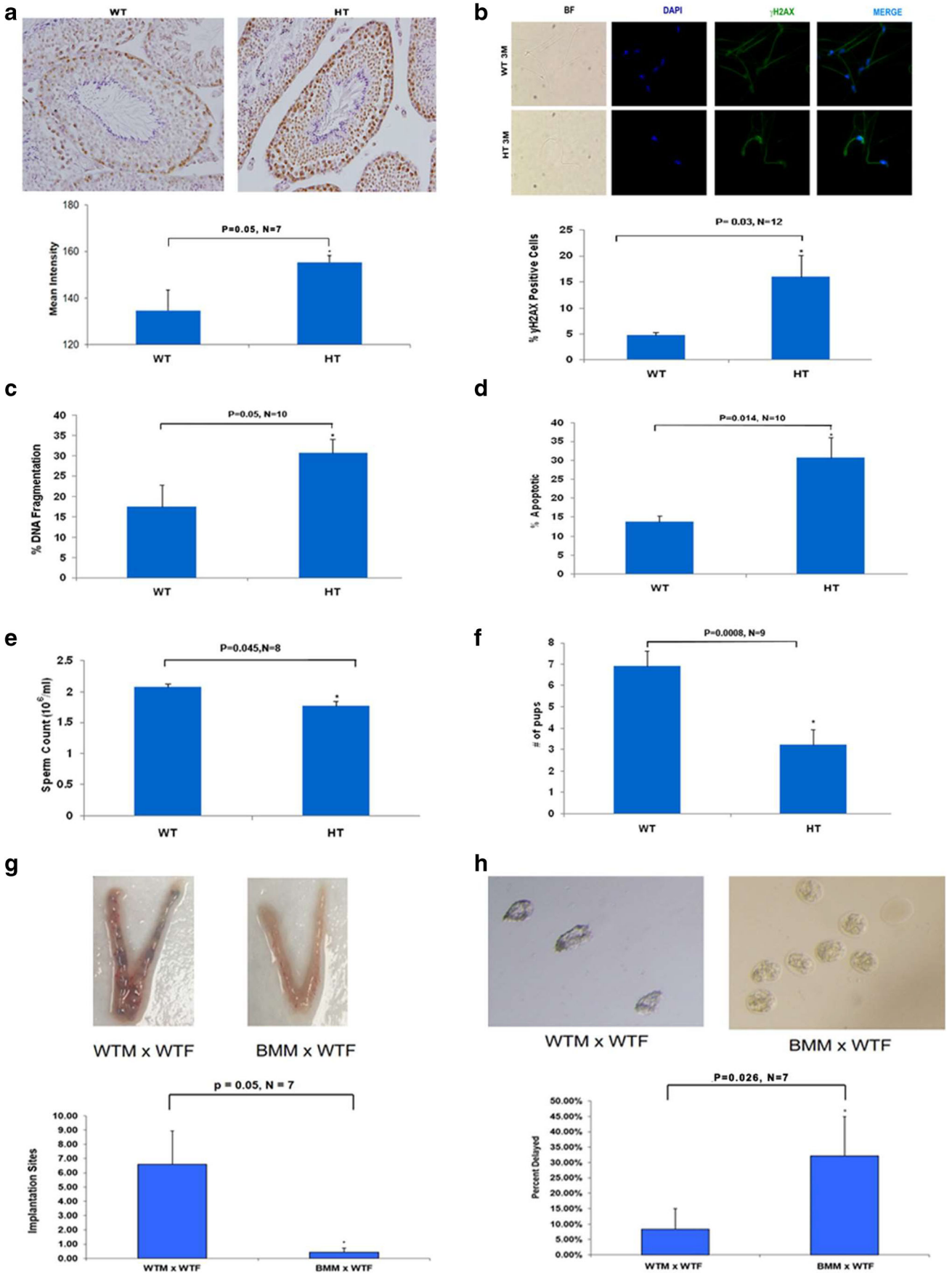
a
WT
HT
Mean Intensity
P=0.05, N=7
b
BF
DAPI
γH2AX
MERGE
WT 3M
HT 3M
% γH2AX Positive Cells
P= 0.03, N=12
c
% DNA Fragmentation
P=0.05, N=10
d
% Apoptotic
P=0.014, N=10
e
Sperm Count (10^6/ml)
P=0.045,N=8
f
# of pups
P=0.0008, N=9
g
WTM x WTF
BMM x WTF
Implantation Sites
p = 0.05, N = 7
h
WTM x WTF
BMM x WTF
Percent Delayed
P=0.026, N=7

◀ **Fig. 3** Increased sperm DNA damage in in haploinsufficient BRCA1 male mouse. **a** Representative photomicrographs show γH2AX staining of haploinsufficient BRCA1 mice testicular tissue at × 40 magnification. Bar graph shows a higher expression of γH2AX as represented by the intensity of the γH2AX immunofluorescence in the spermatogonium and spermatocytes in testicular tissue of haploinsufficient BRCA1 mice testis by laser scanning cytometry (155.2 ± 3.4 vs. 134.6 ± 8.9, $n = 7$; $P = 0.05$, Student's t test). **b** Photomicrographs represent γH2AX foci (green) and counterstaining of DAPI (blue) of sperm cells from young and old WT mice at × 40 magnification. Bar graph shows an increase in DNA damage as reported by γH2AX expression (15.9 ± 4.3 vs. 4.6 ± 0.6, $n = 12$; $P = 0.03$, Student's t test), **c** increased susceptibility of DNA of sperm cells to denaturation by the acridine orange assay (30.6 ± 3.4 vs. 17.4 ± 5.3, $n = 10$; $P = 0.05$, Student's t test), **d** increased percentage of apoptosis via FLICA analysis (30.7 ± 5.4 vs. 13.9 ± 1.5, n = 10; $P < 0.014$, Student's t test), and **e** lower sperm concentration compared to WT ($1.8 \times 10^6 \pm 0.1 \times 10^6$ vs. $2.1 \times 10^6 \pm 0.07 \times 10^6$, $n = 8$; $P = 0.045$, Student's t test). **f** Haploinsufficiency of BRCA1 male mice resulted in smaller litter size when mated with WT females compared to when WT males were mated with WT females (3.2 ± 0.77 vs. 6.9 ± 0.42, $n = 9$; $P = 0.0008$, Student's t test). **g** Representative photomicrographs show implantation sites produced by crossing BRCA1 WT mice with WT females and haploinsufficient BRCA1 male mice with WT females. Bar graph shows implantation sites were significantly decreased in WT females crossed with haploinsufficient BRCA1 male mice (0.43 ± 0.30 vs. 6.60 ± 2.34, $n = 7$; $P = 0.05$, Student's t test) when compared to crossing with WT males. **h** Representative photomicrographs show increased percentage of arrested embryos produced by the crosses mentioned from the implantation sites at × 20 magnification. Bar graph shows a higher percentage of arrested embryos produced by crossing haploinsufficient BRCA1 male mice with WT females (32.14% ± 0.13% vs. 8.33% ± 0.07%, $n = 7$; $P = 0.026$, Student's t test) as compared to WT mice. All results are mean ± SEM

± 0.005 vs. 0.021 ± 0.015, $n = 8$; $P = 0.013$, Student's t test) in the presence of an ATM inhibitor (Fig. S2A–F).

Alkaline and Neutral Comet Assay in S1P-Treated Mouse Sperm With and Without an ATM Inhibitor

To confirm the effects of S1P on sperm DNA DSB repair, we utilized COMET assay as an independent method of DNA damage assessment. Alkaline COMET assay is a generalized assay for DNA breaks while the neutral assay is more specific to DSBs [31]. By COMET assay too, S1P treatment reduced DNA DSBs compared to baseline and genotoxic stress alone. On neutral comet assay, S1P-reduced spontaneous (18.5 ± 0.59 vs. 27.8 ± 0.52, $n = 9$; $P = 0.000018$, Student's t test) and genotoxic stress–induced DNA damage (18.8 ± 0.73 vs. 29.6 ± 0.64, $n = 9$; $P = 0.00004$, Student's t test) (Fig. S3A). Likewise, on alkaline comet assay too, S1P treatment reduced both spontaneous (16.79 ± 0.89 vs. 24.7 ± 0.76, $n = 9$; $P = 0.000093$, Student's t test) and genotoxic stress induced DNA damage (16.8 ± 0.87 vs. 27.3 ± 0.90, $n = 9$; $P = 0.00004$) (Fig. S3C). These beneficial effects of S1P on DNA DSB repair were again blocked by the co-treatment with an ATM inhibitor (Fig. S3B&D), validating the specificity of the actions of S1P on the ATM-mediated DNA DSB repair pathway.

Discussion

In a previous study, we demonstrated that DSB repair and its decline with age is critical in oocyte aging [2]. In the current study, we set out to determine the role of DNA damage and DSB repair in sperm. Our findings from testicular sections showed that expression of γH2AX was significantly increased in spermatogonium and spermatocytes with age. Based on this age-related increase in spermatogonium and spermatocyte damage, we hypothesized that the sperm DNA repair function may decline from the earliest stages of spermatogenesis. We found that DNA repair declined with age in sperm, resulting in the accumulation of DSBs in sperm measured by both γH2AX and COMET assays. This was accompanied by alteration of sperm DNA integrity with age. Further, in haploinsufficient BRCA1 mice, the findings from aged mice were replicated and the embryo development was altered in WT female mice impregnated by haploinsufficient BRCA1 male mice. These findings indicated that DSB repair is critical in sperm quality and function. Moreover, by treating the sperm with a naturally occurring sphingolipid S1P, we were able to enhance DNA repair and reverse aging-associated changes. These findings suggest that DNA repair could be a target for pharmacologically reversing male reproductive aging and enhancing sperm quality.

Earlier studies on sperm DNA integrity mainly focused on DNA fragmentation. Some of those studies showed an association between sperm fragmentation and reduced fertility [32, 33]. Other studies have suggested that DNA fragmentation is another manifestation of intensive DSBs in sperm [34, 35]. However, the reasons behind increased DNA fragmentation in some individuals and its relationship with aging were never explained. Perhaps the complacency towards providing an explanation was the earlier doctrine that sperm were transcriptionally inactive. Prior studies in the male reproductive system only focused on DNA repair in sperm during their time of development in the testes. Some have doubted the presence of DNA repair mechanisms and questioned whether they can play an important role in sperm survival and fertility [36–38].

Other studies, on the other hand, showed that oocytes and early embryos could repair sperm DNA damage, and the impact of sperm DNA fragmentation on embryo development depended on the combined effects of the extent of sperm chromatin damage and the capacity of the oocyte to repair it [39]. In addition, a recent study demonstrated that the zygote responds to sperm DNA damage by slowing paternal DNA replication, which could lead to embryonic arrest [40]. Along with this, Amaral et al. provided a list of all sperm proteins described to date and noted that the functional relevance of several sperm proteins, such as those related to protein synthesis, remains unclear [41].

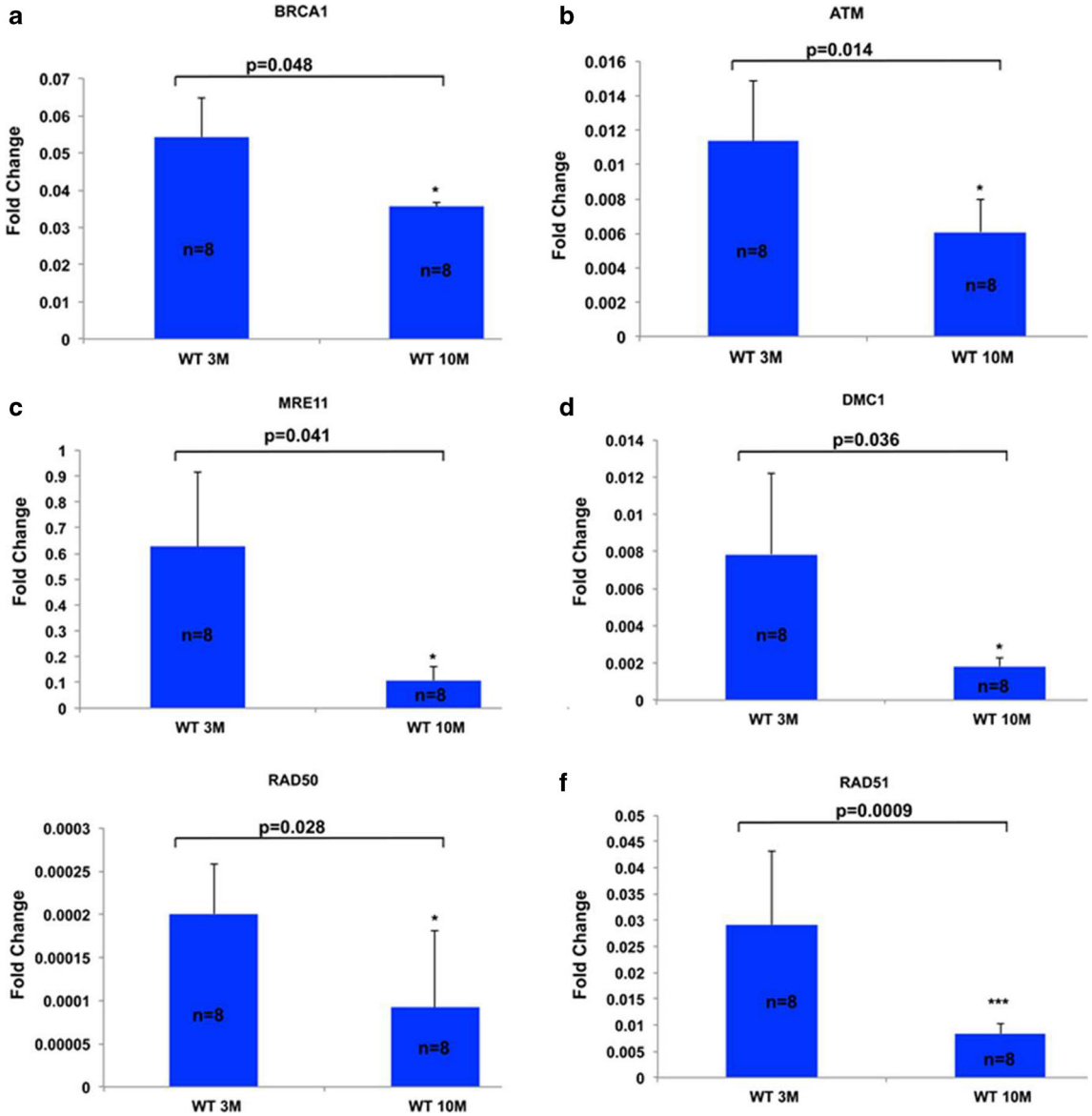

Fig. 4 Age-related decline in the expression of DNA repair genes in mouse sperm. Significant decreases in the expression of DNA repair genes in old WT mice as compared to young shown by real-time PCR. All results are mean ± SEM ($n = 8$ per group). Bar graphs represent the gene expressions, which are significantly lower for key DNA repair genes with age, including **a** BRCA1 (0.05 ± 0.01 vs. 0.04 ± 0.001, $P = 0.048$, Student's t test), **b** ATM (0.011 ± 0.003 vs. 0.006 ± 0.002, $P = 0.014$, Student's t test), **c** MRE11 (0.6 ± 0.3 vs. 0.1 ± 0.05, $P = 0.041$, Student's t test), **d** DMC1 (0.008 ± 0.004 vs. 0.002 ± 0.004, $P = 0.036$, Student's t test), **e** RAD50 ($2.2 \times 10^{-4} \pm 5 \times 10^{-5}$ vs. $9.2 \times 10^{-5} \pm 8 \times 10^{-5}$, $P = 0.028$, Student's t test), and **f** RAD51 (0.3 ± 0.4 vs. 0.01 ± 0.4, $P = 0.0009$, Student's t test)

Studies also addressed the dispute as to whether there is protein synthesis occurring in mature spermatozoa at all, or if the proteins and RNAs found are simply remnants from earlier spermatogenesis [41]. Human sperm contain various transcription factors related to RNA metabolism, however, transcription is limited in human sperm due to limited proteomic machinery needed to perform transcription. Nonetheless, spermatozoa seem to contain proteins involved in RNA metabolism, which includes mRNA degradation pathways as well as packaging and processing of small nuclear ribonucleoproteins [41]. Multiple publications also established that there was a complex population of RNAs in ejaculated human sperm. However, the functional significance of most nuclear-encoded sperm transcripts is yet to be established.

Recent studies do suggest probable roles of a few sperm transcripts, which are related to genome packaging, early embryogenesis, transmission of paternal epigenetic information, and protein translation [41]. Absent from these investigations was the role of DNA repair in sperm, which was addressed in the current study. Our study indicated that the BRCA-related DSB repair genes can be actively transcribed in mature sperm and may play critical functional roles in maintaining sperm

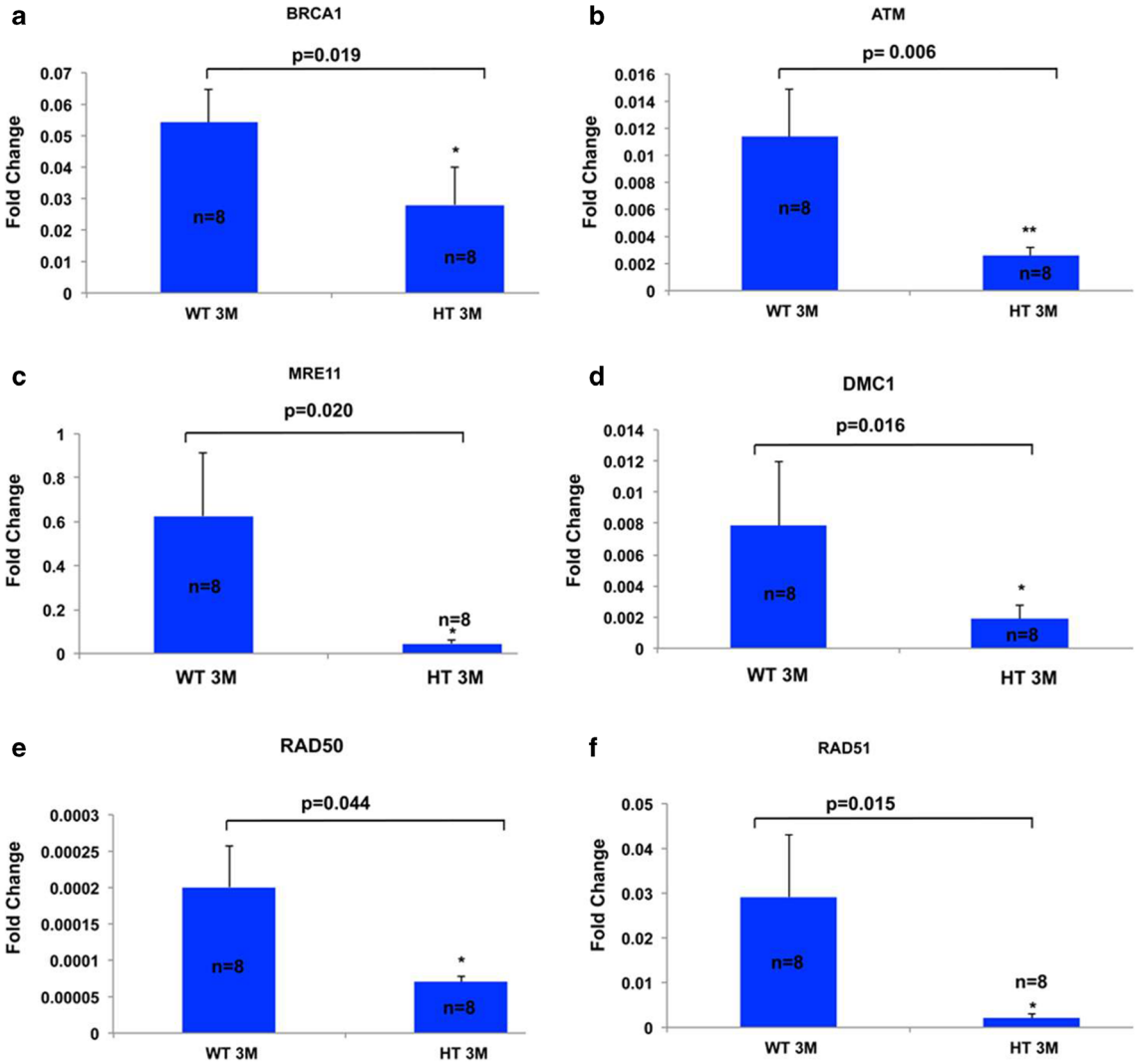

Fig. 5 Compromised sperm DNA repair gene function in haploinsufficient BRCA1 male mouse. All results are mean ± SEM ($n = 8$ per group). Bar graphs represent the expressions of key DNA repair genes by qRT-PCR, which are significantly lower for **a** BRCA1 (0.028 ± 0.012 vs. 0.05 ± 0.01, $P = 0.019$, Student's t test), **b** ATM (0.002 ± 0.0005 vs. 0.011 ± 0.003, $P = 0.006$, Student's t test), **c** MRE11 (0.045 ± 0.018 vs. 0.6 ± 0.3, $P = 0.02$, Student's t test), and **d** DMC1 ($0.002 \pm 9 \times 10^{-4}$ vs. 0.008 ± 0.004, $P = 0.02$, Student's t test), **e** RAD50 ($9.7 \times 10^{-5} \pm 8.9 \times 10^{-6}$ vs. $2.2 \times 10^{-4} \pm 5 \times 10^{-5}$, $P = 0.044$, Student's t test), and **f** RAD51 ($0.002 \pm 8 \times 10^{-4}$ vs. 0.03 ± 0.4, $P = 0.015$, Student's t test) compared to WT.

quality. The altered sperm and embryo quality from haploinsufficient BRCA1 male mice highlights a potential important role for DSB repair in male reproduction. In addition, male infertility has traditionally been diagnosed by microscopic assessment of the sperm in the ejaculate for concentration, and motility, which provided a crude assessment of quality [38]. Our study adds the possibility that the extent of DNA damage and the presence DSBs as well as the BRCA1-mediated DSB repair gene function can potentially be quantified to assess sperm quality.

Another potential clinical implication of our study is for BRCA-mutation carrier men. Starting with our first clinical observations [42] and continuing with our translational work [2, 43], we have provided strong evidence that ovarian aging is accelerated in women with BRCA mutations. This has been confirmed by numerous other studies showing early menopausal age [44, 45], lower serum anti-Mullerian hormone levels [2, 46, 47], and lower primordial follicle density [43] in women with BRCA mutations. Our current study raises the possibility that men with BRCA mutations may also have accelerated reproductive aging. Further clinical studies are warranted to investigate semen quality and reproductive performance in men with BRCA mutations.

Ceramide-induced death pathway has been shown to be instrumental in radiotherapy and chemotherapy-induced oocyte death [15, 16]. S1P, a byproduct of the ceramide-induced pathway, has been shown to block ceramide-induced apoptosis in oocytes ex vivo, triggered by radiotherapy [15] and

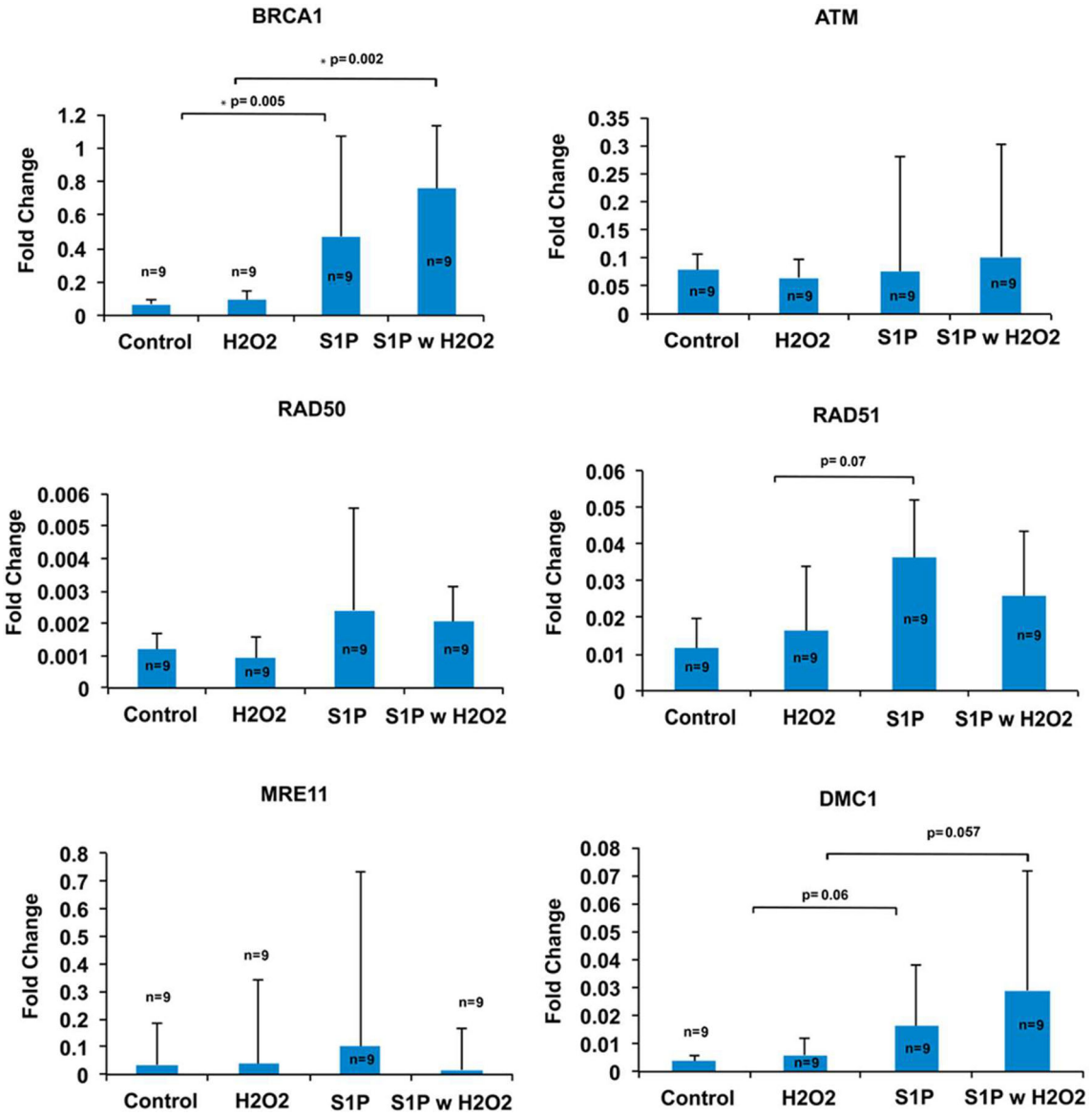

Fig. 6 S1P treatment enhances DNA DSB repair in sperm. S1P treatment induced the expression of BRCA1 compared to baseline (0.471 ± 0.602 vs. 0.068 ± 0.031, $n = 9$; $P = 0.005$, Student's t test) and H_2O_2-treated sperm (0.755 ± 0.377 vs. 0.090 ± 0.053, $n = 9$; $P = 0.002$ Student's t test). Furthermore, there was a trend for increase in the expression of Rad51 (0.036 ± 0.015 vs. 0.012 ± 0.008, $n = 9$; $P = 0.07$, Student's t test) and DMC1 (0.016 ± 0.02 vs. 0.003 ± 0.002, $n = 9$; $P = 0.06$, Student's t test) in the S1P treated samples when compared to the controls. Other genes tested showed no significant difference in the S1P treated sperm when compared to the control. All results are mean ± SEM

chemotherapy [16]. In an in vivo xenograft model, our laboratory showed that S1P blocked doxorubicin and cyclophosphamide-induced primordial follicle death in human ovarian tissue. Since we showed that chemotherapy induced oocyte death by causing DSBs [48], we hypothesized that S1P may prevent chemotherapy-induced germ cell DNA damage and death by enhancing DNA repair. Based on that hypothesis, we tested S1P's ability to enhance DNA repair in sperm. A different study observed that ghrelin administration prevents cisplatin-induced germ cell damage through demonstrating decreased sperm DNA damage by enhanced DNA repair mechanisms [49]. This finding further indicates the importance of DNA repair in sperm.

In our study, sperm from young WT mice were treated with S1P alone and with an ATM inhibitor, and analyzed for DNA damage, apoptosis, and chromatin integrity. There was a significant decrease in DNA damage when sperm was treated with S1P under genotoxic stress. S1P treatment reversed DNA damage induced by H_2O_2 exposure as shown both by γH2AX and COMET assays. The ATM specificity of this effect was shown via the abrogation of the DNA repair enhancing effects of S1P by ATM-inhibitor treatment. The

reduction in DSBs occurred by enhancing DNA repair with S1P, however, other etiologies would need to be investigated to further confirm these findings.

In congregate, these findings suggest a strong role for DNA damage repair in maintenance of sperm quality. Our study also shows a possible pharmaceutical approach to prevent sperm aging. Further in vivo animal and translational studies in aging men as well as those in BRCA mutation carriers are warranted to affirm the clinical significance of our findings.

Author Contributions K.O. conceived the idea and designed and directed the study; R.S. and S.T. performed the laboratory experiments and statistical analysis; D.H. and Z.D. measured and analyzed samples for flow cytometry and laser scanning cytometry; R.S. wrote the initial draft of the manuscript; and K.O., S.T., Z.D., D.H. reviewed and edited the manuscript.

Funding Information NIH Grant R01 HD053112 to K.O. partially supported this work.

Compliance with Ethical Standards

Competing Interest The authors declare that they have no competing interests.

References

1. Herbert M, Kalleas D, Cooney D, Lamb M, Lister L. Meiosis and maternal aging: insights from aneuploid oocytes and trisomy births. Cold Spring Harb Perspect Biol. 2015;7(4):a017970.
2. Titus S, Li F, Stobezki R, et al. Impairment of BRCA1-related DNA double-strand break repair leads to ovarian aging in mice and humans. Sci Transl Med. 2013;5(172):172ra121.
3. Kuhnert B, Nieschlag E. Reproductive functions of the ageing male. Hum Reprod Update. 2004;10(4):327–39.
4. Johnson SL, Dunleavy J, Gemmell NJ, Nakagawa S. Consistent age-dependent declines in human semen quality: a systematic review and meta-analysis. Ageing Res Rev. 2015;19:22–33.
5. Belloc S, Benkhalifa M, Cohen-Bacrie M, Dalleac A, Amar E, Zini A. Sperm deoxyribonucleic acid damage in normozoospermic men is related to age and sperm progressive motility. Fertil Steril. 2014;101(6):1588–93.
6. Templado C, Bosch M, Benet J. Frequency and distribution of chromosome abnormalities in human spermatozoa. Cytogenet Genome Res. 2005;111(3–4):199–205.
7. Sikka SC. Oxidative stress and role of antioxidants in normal and abnormal sperm function. Front Biosci. 1996;1:e78–86.
8. Ramasamy R, Chiba K, Butler P, Lamb DJ. Male biological clock: a critical analysis of advanced paternal age. Fertil Steril. 2015;103(6):1402–6.
9. Stewart AF, Kim ED. Fertility concerns for the aging male. Urology. 2011;78(3):496–9.
10. Schmid TE, Eskenazi B, Baumgartner A, Marchetti F, Young S, Weldon R, et al. The effects of male age on sperm DNA damage in healthy non-smokers. Hum Reprod. 2007;22(1):180–7.
11. Singh NP, Muller CH, Berger RE. Effects of age on DNA double-strand breaks and apoptosis in human sperm. Fertil Steril. 2003;80(6):1420–30.
12. Sartorius GA, Nieschlag E. Paternal age and reproduction. Hum Reprod Update. 2010;16(1):65–79.
13. Harris ID, Fronczak C, Roth L, Meacham RB. Fertility and the aging male. Reviews in Urology. 2011;13(4):e184–90.
14. Sauer MV. Reproduction at an advanced maternal age and maternal health. Fertil Steril. 2015;103(5):1136–43.
15. Morita Y, Perez GI, Paris F, Miranda SR, Ehleiter D, Haimovitz-Friedman A, et al. Oocyte apoptosis is suppressed by disruption of the acid sphingomyelinase gene or by sphingosine-1-phosphate therapy. Nat Med. 2000;6(10):1109–14.
16. Li F, Turan V, Lierman S, Cuvelier C, De Sutter P, Oktay K. Sphingosine-1-phosphate prevents chemotherapy-induced human primordial follicle death. Hum Reprod. 2014;29(1):107–13.
17. Shen SX, Weaver Z, Xu X, Li C, Weinstein M, Chen L, et al. A targeted disruption of the murine Brca1 gene causes gamma-irradiation hypersensitivity and genetic instability. Oncogene. 1998;17(24):3115–24.
18. Huber LJ, Yang TW, Sarkisian CJ, Master SR, Deng CX, Chodosh LA. Impaired DNA damage response in cells expressing an exon 11-deleted murine Brca1 variant that localizes to nuclear foci. Mol Cell Biol. 2001;21(12):4005–15.
19. Lane M, McPherson NO, Fullston T, Spillane M, Sandeman L, Kang WX, et al. Oxidative stress in mouse sperm impairs embryo development, fetal growth and alters adiposity and glucose regulation in female offspring. PLoS One. 2014;9(7):e100832.
20. Katsube T, Mori M, Tsuji H, Shiomi T, Wang B, Liu Q, et al. Most hydrogen peroxide-induced histone H2AX phosphorylation is mediated by ATR and is not dependent on DNA double-strand breaks. J Biochem. 2014;156(2):85–95.
21. Halicka D, Ita M, Tanaka T, Kurose A, Darzynkiewicz Z. Biscoclaurine alkaloid cepharanthine protects DNA in TK6 lymphoblastoid cells from constitutive oxidative damage. Pharmacological reports : PR. 2008;60(1):93–100.
22. Hawley TS, Hawley RG. Flow cytometry protocols. 2nd ed. Totowa, N.J: Humana Press; 2004.
23. Evenson DP, Darzynkiewicz Z, Melamed MR. Relation of mammalian sperm chromatin heterogeneity to fertility. Science. 1980;210(4474):1131–3.
24. Bedner E, Smolewski P, Amstad P, Darzynkiewicz Z. Activation of caspases measured in situ by binding of fluorochrome-labeled inhibitors of caspases (FLICA): correlation with DNA fragmentation. Exp Cell Res. 2000;259(1):308–13.
25. Darzynkiewicz Z, Pozarowski P, Lee BW, Johnson GL. Fluorochrome-labeled inhibitors of caspases: convenient in vitro and in vivo markers of apoptotic cells for cytometric analysis. *Methods in molecular biology (Clifton, NJ).* 2011;682:103–114.
26. Rio DC, Ares M, Jr., Hannon GJ, Nilsen TW. Purification of RNA using TRIzol (TRI reagent). *Cold Spring Harb Protoc.* 2010;2010(6):pdb prot5439.
27. Smart DJ, Halicka HD, Schmuck G, Traganos F, Darzynkiewicz Z, Williams GM. Assessment of DNA double-strand breaks and gammaH2AX induced by the topoisomerase II poisons etoposide and mitoxantrone. Mutat Res. 2008;641(1–2):43–7.
28. Williams GM, Duan JD, Brunnemann KD, Iatropoulos MJ, Vock E, Deschl U. Chicken fetal liver DNA damage and adduct formation by activation-dependent DNA-reactive carcinogens and related compounds of several structural classes. Toxicol Sci. 2014;141(1):18–28.
29. Russ JC. The image processing handbook. 2nd ed. Boca Raton: CRC Press; 1995.
30. Gorczyca W, Traganos F, Jesionowska H, Darzynkiewicz Z. Presence of DNA strand breaks and increased sensitivity of DNA in situ to denaturation in abnormal human sperm cells: analogy to apoptosis of somatic cells. Exp Cell Res. 1993;207(1):202–5.
31. Ribas-Maynou J, Garcia-Peiro A, Fernandez-Encinas A, et al. Comprehensive analysis of sperm DNA fragmentation by five different assays: TUNEL assay, SCSA, SCD test and alkaline and neutral comet assay. Andrology. 2013;1(5):715–22.

32. Muratori M, Marchiani S, Tamburrino L, Tocci V, Failli P, Forti G, et al. Nuclear staining identifies two populations of human sperm with different DNA fragmentation extent and relationship with semen parameters. Hum Reprod. 2008;23(5):1035–43.
33. Chan PJ, Corselli JU, Patton WC, Jacobson JD, Chan SR, King A. A simple comet assay for archived sperm correlates DNA fragmentation to reduced hyperactivation and penetration of zona-free hamster oocytes. Fertil Steril. 2001;75(1):186–92.
34. Ribas-Maynou J, Garcia-Peiro A, Fernandez-Encinas A, et al. Double stranded sperm DNA breaks, measured by comet assay, are associated with unexplained recurrent miscarriage in couples without a female factor. PLoS One. 2012;7(9):e44679.
35. Garolla A, Cosci I, Bertoldo A, Sartini B, Boudjema E, Foresta C. DNA double strand breaks in human spermatozoa can be predictive for assisted reproductive outcome. Reprod BioMed Online. 2015;31(1):100–7.
36. Leduc F, Nkoma GB, Boissonneault G. Spermiogenesis and DNA repair: a possible etiology of human infertility and genetic disorders. Syst Biol Reprod Med. 2008;54(1):3–10.
37. Lalancette C, Miller D, Li Y, Krawetz SA. Paternal contributions: new functional insights for spermatozoal RNA. J Cell Biochem. 2008;104(5):1570–9.
38. Gonzalez-Marin C, Gosalvez J, Roy R. Types, causes, detection and repair of DNA fragmentation in animal and human sperm cells. Int J Mol Sci. 2012;13(11):14026–52.
39. Derijck A, van der Heijden G, Giele M, Philippens M, de Boer P. DNA double-strand break repair in parental chromatin of mouse zygotes, the first cell cycle as an origin of de novo mutation. Hum Mol Genet. 2008;17(13):1922–37.
40. Gawecka JE, Marh J, Ortega M, Yamauchi Y, Ward MA, Ward WS. Mouse zygotes respond to severe sperm DNA damage by delaying paternal DNA replication and embryonic development. PLoS One. 2013;8(2):e56385.
41. Amaral A, Castillo J, Ramalho-Santos J, Oliva R. The combined human sperm proteome: cellular pathways and implications for basic and clinical science. Hum Reprod Update. 2014;20(1):40–62.
42. Oktay K, Kim JY, Barad D, Babayev SN. Association of BRCA1 mutations with occult primary ovarian insufficiency: a possible explanation for the link between infertility and breast/ovarian cancer risks. J Clin Oncol. 2010;28(2):240–4.
43. Lin W, Titus S, Moy F, Ginsburg ES, Oktay K. Ovarian aging in women with BRCA germline mutations. J Clin Endocrinol Metab. 2017;102(10):3839–47.
44. Lin WT, Beattie M, Chen LM, Oktay K, Crawford SL, Gold EB, et al. Comparison of age at natural menopause in BRCA1/2 mutation carriers with a non-clinic-based sample of women in Northern California. Cancer. 2013;119(9):1652–9.
45. Oktay K, Moy F, Titus S, Stobezki R, Turan V, Dickler M, et al. Age-related decline in DNA repair function explains diminished ovarian reserve, earlier menopause, and possible oocyte vulnerability to chemotherapy in women with BRCA mutations. J Clin Oncol. 2014;32(10):1093–4.
46. Wang Y, Feng G, Wang J, Zhou Y, Liu Y, Shi Y, et al. Differential effects of tumor necrosis factor-alpha on matrix metalloproteinase-2 expression in human myometrial and uterine leiomyoma smooth muscle cells. Hum Reprod. 2015;30(1):61–70.
47. Ben-Aharon I, Levi M, Margel D, Yerushalmi R, Rizel S, Perry S, et al. Premature ovarian aging in BRCA carriers: a prototype of systemic precocious aging? Oncotarget. 2018;9(22):15931–41.
48. Soleimani R, Heytens E, Oktay K. Enhancement of neoangiogenesis and follicle survival by sphingosine-1-phosphate in human ovarian tissue xenotransplants. PLoS One. 2011;6(4):e19475.
49. Garcia JM, Chen JA, Guillory B, Donehower LA, Smith RG, Lamb DJ. Ghrelin prevents cisplatin-induced testicular damage by facilitating repair of DNA double strand breaks through activation of p53 in mice. Biol Reprod. 2015;93(1):24.